New Mechanism for Autoxidation of polyolefins: kinetic Monte Carlo Modelling of the Role of Short-chain Branches, Molecular Oxygen and Unsaturated Moieties

Lies De Keer,[1] Paul Van Steenberge,[1,*] Marie-Francoise Reyniers[1]

[1]Department of Materials, Textiles and Chemical Engineering, Laboratory for Chemical Technology, Ghent University, Technologiepark 125, 9052 Zwijnaarde, Belgium

Ganna Gryn'ova,[2,3] Heather M. Aitken,[2] Michelle L. Coote[2,*]

[2]ARC Centre of Excellence for Electromaterials Science, Research School of Chemistry, Australian National University, Canberra, Australian Capital Territory, 2601, Australia

[3]Heidelberg Institute for Theoretical Studies (HITS gGmbH), and Interdisciplinary Center for Scientific Computing (IWR), Heidelberg University, Heidelberg, Germany

ABSTRACT:

In this work, a bivariate kinetic Monte Carlo (*k*MC) model is constructed to study autoxidation, which is the degradation of polymers in the presence of oxygen. The use of computational methods for the determination of rate coefficients as input for the model is illustrated. Focus is on the presence of short-chain branches (SCB) and unsaturated moieties and their role in the fate of alkyl, alkoxyl and alkylperoxyl radicals in the autoxidation mechanism. To answer this, the autoxidation kinetics are studied for three model polymers, namely poly(ethylene) (reference case), poly(butadiene) (presence of allylic hydrogens), and poly(isobutylene) (presence of quaternary carbon atoms). Using the *k*MC model, reaction path analysis shows that the autoxidation mechanism for each of the polymer types follows a chain reaction mechanism, but that the presence of branches/unsaturated moieties influences the dominant reaction pathway in the autoxidation mechanism, and thus also the autoxidation rate. It is shown that the influence of varying oxygen concentration and initiation rate coefficient (e.g. to simulate variable ultraviolet (UV) light intensity) on the dominant pathway is small as their role is mainly situated in the first steps of the chain mechanism.

INTRODUCTION

Environmental pollution by solid plastic waste is a serious societal challenge. A step towards addressing this problem is obtaining a better understanding of polymer degradation. Depending on the application, this is useful in the design of more inherently stable polymers to reduce waste, or conversely, more inherently degradable polymers. It can also help assessing whether laboratory-based accelerated ageing experiments are indicative of environmental degradation.[1]

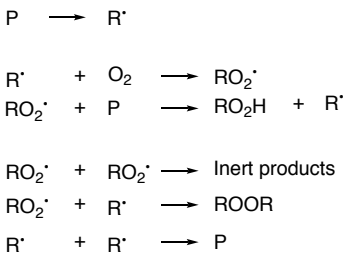

Scheme 1. Basic chain reaction mechanism for autoxidation, developed by Bolland and Gee (called basic autoxidation scheme, BAS);[2-6] P = dead polymer chain; R• = polymer alkyl radical; RO_2• = polymer alkylperoxyl radical.

The textbook mechanism for polymer degradation in the presence of oxygen, so-called autoxidation (Scheme 1), published 70 years ago and also called the basic autoxidation scheme (BAS).[2-7] It was derived for the specific case of lipids and rubbers, but has since been assumed to be universally valid.[8, 9] This is despite the fact that the key propagation reaction in the mechanism, namely hydrogen abstraction from one polymer chain by another polymeric peroxyl radical (ROO•), while favourable for the allylic hydrogen atoms in unsaturated polymers is highly unfavourable for most types of polymers.[10]

To solve this riddle, Coote and co-workers have studied how reactive oxygen species interact with polymers,[11-13] and have re-examined literature observations in the light of these results.[14] Based on this work, it appears that several factors influence autoxidation behaviour including:

- the presence or absence of unsaturated groups as repeat units or defects. For these groups, the peroxyl hydrogen abstraction reaction is favoured, but for most other groups it is not.[10]
- the presence or absence of tertiary/quaternary carbons as repeat units or defects (*e.g.* branches). When these are present peroxyl termination leads primarily

to reactive alkoxy species, whereas when they are absent peroxyl termination leads to non-radical products.[13]

- the presence or absence of oxygen, particularly when branches and unsaturated groups are absent. In those cases carbon-centred propagating radicals are capable of hydrogen abstraction but in the presence of oxygen these are rapidly converted to less reactive peroxyl radicals.[14]

In support of these findings, there is extensive experimental literature showing that the presence of branches and unsaturated groups as defects, formed as a result of side-reactions that arise during polymerization, degradation and curing, detrimentally impact polymer stability.[15, 16] Moreover, studies have also shown that polymer degradation actually increases in an inert atmosphere versus air, under otherwise identical conditions.[17-19] Thus, it seems likely the propagation of autoxidation depends on the nature of the propagating species, which in turn depends on the chemical structure of the degrading polymer and the presence or absence of oxygen (Scheme 2).

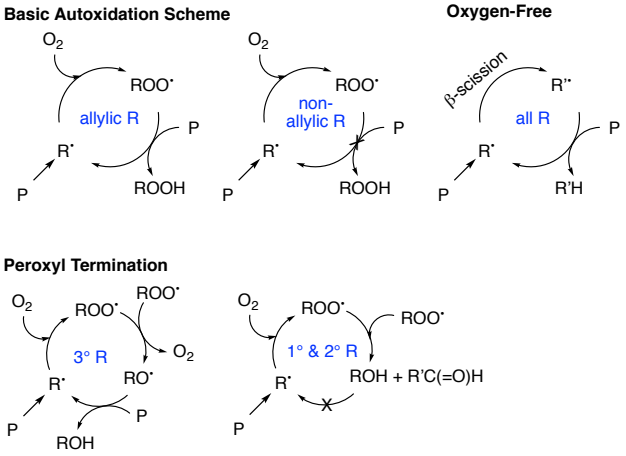

Scheme 2. Alternative propagation mechanisms based on the nature of the propagating species.

However, a missing piece in the autoxidation puzzle is the role of kinetics. It is almost certain that the radical flux plays an important role in whether, for example peroxyl radicals undergo propagation as per the Boland and Gee scheme[2-6] or termination, which conflicts with this scheme. Moreover, this is also key to understanding whether accelerated ageing,[20-24] which involves a high rate of radical initiation (*e.g.* by high ultraviolet (UV) light intensity) proceeds via the same mechanism as environmental degradation, where the initiation rate is much lower.

In present work, we develop a kinetic Monte Carlo (*k*MC) model of polymer autoxidation to examine whether and under what conditions autoxidation occurs via the standard Boland and Gee scheme[2-6] versus the alternative mechanisms proposed. Previous work has shown that chemical kinetics can be simulated via *k*MC in a straight-forward way using Gillespie's stochastic simulation algorithm (SSA).[25, 26] The SSA was initially developed for reactions of elemental species but has been extended to both polymerization and degradation of polymers. In particular, binary trees are efficient data structures to represent chain length distributions of homopolymer molecules,[27] while composite binary trees can also represent chemical composition (*e.g.* double bonds) or branching.[28]Herein, we simulate autoxidation via a *k*MC model that uses bivariate tree data structures[27, 28] to store polymer distributions according to both chain length (first variate) and the number of defects (second variate).

To build our *k*MC model, we make use of literature values for the rate coefficients of each individual reaction, supplemented where necessary by first principles calculations. Three limiting case studies are considered (Table 1). These comprise poly(ethylene) (PE), poly(butadiene) (PBD) and poly(isobutylene) (PIB), which feature degrading species that differ according to whether the radical is stabilized by an allylic double bond (PBD) or not (PE, PIB), and in the latter case whether tertiary radicals are present (PIB) or not (PE). PE is thus considered as reference case and PBD and PIB are considered to assess the effect of unsaturated and branched moieties on the kinetics respectively. The significance of the first distinction (PBD *vs.* PE/PIB) is that for PBD, the peroxyl H-abstraction reaction is favourable, while for the others, it is strongly thermodynamically disfavoured. The key difference between the second distinction (PE vs. PIB) is the outcome of the peroxyl radical termination reaction, with PE giving rise to non-radical products and PIB giving rise to reactive alkoxy radicals (RO•). This differing pattern of behaviour is archetypal of polymers that propagate via primary or secondary carbon-centred radicals (PE) versus those that propagate via tertiary carbon-centred radicals (PIB).

Table 1. Model polymers considered in this work.

Polymer Type	***Repeat unit***	***Propagating species***	***Peroxyl fate***[(*),(**)]	
Polyethylene (PE)	CH_2CH_2	$–CH_2CH_2•$	$2RO_2• \rightarrow 2RO• + O_2$	$k = 0$
			$2RO_2• \rightarrow$ R'C(O)R" + ROH + O_2	$k \neq 0$
			$RO_2• + P \leftrightarrows ROOH + R•$	$k \approx 0$
Polybutadiene (PBD)	$CH_2CH=CHCH_2$	$–CH=CHCH_2•$	$2RO_2• \rightarrow 2RO• + O_2$	$k = 0$
			$2RO_2• \rightarrow$ R'C(O)R" + ROH + O_2	$k \neq 0$
			$RO_2• + P \leftrightarrows ROOH + R•$	$k \neq 0$
Polyisobutylene (PIB)	$CHC(CH_3)_2$	$–CH_2C(CH_3)_2•$	**$2RO_2• \rightarrow 2RO• + O_2$**	$k \neq 0$
			$2RO_2• \rightarrow$ R'C(O)R" + ROH + O_2	$k = 0$
			$RO_2• + P \leftrightarrows ROOH + R•$	$k \approx 0$

(*)P = dead polymer chain; R• = polymer alkyl radical; RO• = polymer alkoxyl radical; RO_2• = polymer alkylperoxyl radical;(**)polymer aldehyde (RC(O)H) instead of polymer ketone (R'C(O)R'') in case R is an endchain radical.

By simulating and comparing these different scenarios, we can answer the following questions: (a) "Does the normal propagation step in the BAS still occur for saturated polymers in spite of it being thermodynamically disfavoured?"; (b) "Is peroxyl termination in competition with the peroxyl transfer and even dominant depending on the polymer structure?"; (c) "Does oxygen help to promote or inhibit degradation?"; (d) "To what extent does the mechanism depend on the initiation rate?". Establishing the correct dominant pathway in the autoxidation mechanism under given conditions is important for designing optimal stable polymers or readily degradable ones.

METHODS

Rate Coefficients. Tables S4 to S6 in Supporting Information summarize the rate coefficients used in the *k*MC simulations. Rate coefficients are assumed to be independent of polymer chain length and are sourced from a combination of literature and *ab initio* calculations performed in this work (see Table S1 to S3) for hydrogen abstraction reactions involving R$^\bullet$, RO$^\bullet$ and RO$_2^\bullet$ radicals, dependent on the structure of R being a primary/secondary, tertiary or allylic radical. Historically, rate coefficients for autoxidation modelling have been mainly obtained from fitting of experimental data to the BAS. However, in this work we preferred to obtain parameters (independently from the model) by using quantum-chemical calculations.

Quantum Chemistry. Standard ab initio molecular orbital theory and density functional theory calculations were performed using Gaussian 2016 RevC.01, and MOLPRO 2019.2. Geometry optimisations and frequency computations under harmonic oscillator approximation were performed at the M06-2X/6-31+G(d,p) level of theory. To ensure each geometry was close to a global minimum, all geometries were conformer searched at 120° resolution using the energy directed tree search algorithm.[29] Single point energies were computed using the high level composite *ab initio* method G3(MP2)CC.[30] Standard textbook equations based on the statistical thermodynamics of an ideal gas under the harmonic oscillator and rigid rotor approximation, were used to determine the thermal and entropic corrections at 298 K which contribute to the Gibbs free energies. Frequencies and thermochemical corrections at 298 K were scaled by the recommended scaling factors.[31] Rate constants at 298 K were computed using transition state theory with Eckart tunnelling corrections. Table S1 to S3 in Supporting Information, show respectively the computed H abstraction rate coefficients, the corresponding total energies, entropies and thermal corrections, and the Gaussian archive entries.

Modelling framework. The reactions implemented in the *k*MC model are summarized in Scheme 3 and Tables S4 to S6 in Supporting Information. No polymer additives such as stabilizers are considered. In the *k*MC model, initiation is modelled as a single reaction, although in reality it might require multiple reaction steps, and occur via a variety of mechanisms, *e.g.* photocleavage (under UV irradiation) or thermal decomposition (important during curing of polymers). The simplification is made here because the focus is on understanding the propagation mechanism as a function of the initiation rate. Studies focusing on understanding the homolysis and the subsequent radical rearrangement, involving *e.g.* the release of gaseous product such as CO_2,[32] and fragmentation can be found in literature.[33, 34]

The original polymer chains and the termination products formed during autoxidation are lumped into a single dead species population to select the reactant for initiation, hence no differentiation in initiation rate coefficient is made depending on the chemical structure of these dead species. It is assumed that all non-radical products may undergo initiation randomly along the polymer backbone. Norrish reactions for homolysis of aldehydes/ketones under UV exposure[35] are not accounted for. The alkyl radicals formed upon initiation are scavenged by oxygen to form a peroxyl radical. This reaction is fast and not considered to be the rate-determining step in the propagation phase of the autoxidation mechanism.[36, 37] The decomposition of hydroperoxide chains (ROOH) to form hydroxyl radicals, *i.e.* chain branching, is not accounted for in the model. This decomposition of ROOH is extremely disfavoured, therefore in the absence of a thermodynamically driving force, this reaction is unlikely to be kinetically important.[38]

$P \rightarrow R^\bullet$	Initiation
$R^\bullet + O_2 \rightarrow RO_2^\bullet$ $RO_2^\bullet + P \rightleftarrows ROOH + R^\bullet$ $RO^\bullet + P \rightleftarrows ROH + R^\bullet$ $R^\bullet + P \rightleftarrows P + R^\bullet$ $2RO_2^\bullet \rightarrow 2RO^\bullet + O_2$	Propagation
$R^\bullet \rightarrow P + R^\bullet$	β-scission
$RO_2^\bullet + RO_2^\bullet \rightarrow RC(O)R + ROH + O_2$ $RO_2^\bullet + R^\bullet \rightarrow ROOR$ $R^\bullet + R^\bullet \rightarrow P$	Termination

Scheme 3. Extended chain reaction mechanism for autoxidation (compared to Scheme 1) with added reactions shown in blue; P = dead polymer chain; R$^\bullet$ = polymer alkyl radical; RO$^\bullet$ = polymer alkoxyl radical; RO$_2^\bullet$ = polymer alkylperoxyl radical (in the first termination reaction, a polymer aldehyde is formed instead of a polymer ketone if R is an endchain radical).

A distinction is made between various populations of radicals based on their endgroups (see Figure S3 in Supporting Information). For each population, a bivariate binary tree is defined in the model, tracking its distributed properties. Molecules inside each population are characterized by two stochastic variables: (i) the carbon number of the polymer backbone (CN) and (ii) the number of defects (= allylic or quaternary carbon atoms). The resulting joint, *i.e.* bivariate, chain length-defect distribution of each population is represented in a composite binary tree as shown in Section S2 in Supporting Information. Note that the use of bivariate trees in this work is in fact not really necessary as for the model polymers PBD and PIB considered, it is assumed that each repeating unit contains a defect. However as, in future work, the goal is to study the autoxidation kinetics of polymers with a random distribution of defects, the concept of bivariate trees is already introduced here.

A distinction is further made between reactions of macromolecules with one reactive centre (*e.g.* propagation and recombination), and reactions involving macromolecules with multiple reactive centres (*e.g.* hydrogen abstraction). The first type of reactions obeys a rate law proportional with the concentrations of the reaction partners and can easily be modelled using conventional number-weighted trees (or number binary trees). However, the second type of reaction features reactions occurring on specific sites along polymer backbones involving many reactive centres

per polymer molecule. Hence, their rate law (and reaction probability) is not proportional to the number of involved molecules but rather to the number of involved reaction centres in a single molecule. This second case is special because larger macromolecules have a larger probability to undergo hydrogen abstraction reactions compared to smaller molecules. Hence, the rate laws for this second type of reactions are treated using so-called "mass-weighted" binary trees (or mass binary trees) (see Section S2 in Supporting Information for an example).[39]

Keeping in mind the illustrative nature of this work, the initial polymer distribution for each polymer type (PE, PBD and PIB) is assumed by a Flory Schulz distribution (Eq. (1); Figure 1a):

$$f_{n,i} = \frac{1}{x_n} exp\left(-\frac{i}{x_n}\right) \quad (1)$$

in which $f_{n,i}$ represents the number fraction of polymer chains with a chain length *i,* and x_n is the average chain length of the distribution (taken as 250).

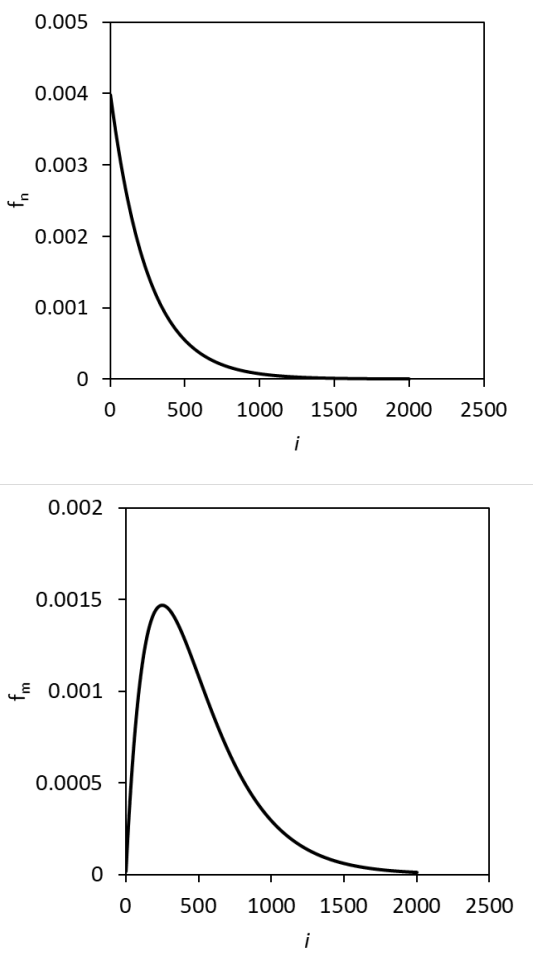

Figure 1. Chain length distribution (CLD) of initial polymer: **(top)** on number fraction basis $f_{n,i}$ and **(bottom)** on mass fraction basis f_{mi}; *i* represents the chain length. The initial distributions based on carbon number are given in Figure S4 in Supporting Information.

For the *k*MC algorithm to sample hydrogen abstraction reactions, this same distribution can be expressed (Figure 1b) in terms of mass fractions. This shows that the peak of the mass chain length distribution is situated at *i* = 250, which is the chain length most statistically likely to undergo hydrogen abstraction. In the *k*MC model, polymer populations are stored based on the carbon number as C-C scission, which in the initiation reaction in the autoxidation mechanism happens due to *e.g.* UV energy, can take place at each position along the polymer backbone.

The reference oxygen concentration, $[O2]_0$, is set at 0.006 mol L^{-1}. This value is based on the oxygen solubility in the polymer at standard temperature and pressure, which is affected by polymer crystallinity and temperature. A range of literature values for PE[40], PP[41] and PBD[42] were averaged, so as to obtain a final value of $[O2]_0$ = 0.006 mol L^{-1}, and sensitivity analysis in which this value was increased by a factor of 100 was also performed. Autoxidation is modelled in a polymer surface layer, where the oxygen is continually replenished from air, hence no O_2 concentration gradients are accounted for (constant O_2 concentration as a function of time).

RESULTS AND DISCUSSION

Using the aforementioned framework, a *k*MC model of autoxidation was constructed according to Scheme 3 and applied to the autoxidation of poly(butadiene) which comprises double bond per repeating unit, of poly(ethylene) which has no defects in its polymer structure, and of poly(isobutylene) which comprises a quaternary C atom per repeating unit. In what follows, the three model polymers considered are treated separately, and thereafter a short comparison between them is given. For every polymer structure, the simulation results with respect to reaction rates of the individual reactions are summarized and following this information, reaction path analysis is applied to determine the dominant reaction pathway. In Figure S5 to S7 in Supporting Information, it is confirmed that for all three model polymers, the autoxidation mechanism is a chain reaction, as the total initiation rate is equal to the total termination rate meaning that no accumulation of radicals is observed. Only 0, 1 or 2 radical(s) exist at each time, as shown in the concentration profiles of the alkyl radicals.

Poly(butadiene) (PBD). For poly(butadiene), the reaction scheme and rate coefficients, as summarized in Table S4 in Supporting Information, are implemented in the *k*MC model. The reaction rates of the competitive reactions are summarized in Table 2 (see Figure S8 and S9 of the Supporting Information for full details). For PBD, two radical types are present in the autoxidation mechanism, allylic end- and allylic midchain radicals. The highest reaction rate for both radical types is obtained for the hydrogen transfer reaction of their $RO_2^{\bullet}$ radicals, which is also the dominant reaction as considered in the BAS. The peroxyl termination rates for these radicals are however only a factor 10 slower than the propagation rates.

In Figure 2, the reaction scheme (for one polymer chain) is summarized. The dominant reaction pathway (composed of initiation/propagation/termination) is indicated by the thicker arrows and exists of the following reaction steps. Allylic endchain radicals are formed via homolysis and react with oxygen to form peroxyl radicals (first two yellow thick arrows at the top). The peroxyl radicals then mostly undergo H abstraction reactions with the formation of midchain allyl radicals (first vertical green thick arrow facing downwards). The midchain allyl radicals react with oxygen (second vertical green thick arrow facing downwards) and their peroxyl radicals also mainly undergo H abstraction reactions (oblique green thick arrow facing upwards). Termination occurs almost exclusively by recombination of

peroxyl radicals (last yellow thick arrow at the bottom). It can thus be seen that polymers with unsaturated moieties follow the BAS for autoxidation as the dominant pathway includes hydrogen abstraction reactions of the peroxyl radicals.

Table 2. Summary of *k*MC model output related to reaction rates (mol L^{-1} s^{-1}) of competitive reactions for poly(butadiene); reaction rate profiles as a function of time are given in Figure S8 and S9 in Supporting Information; red: lowest reaction rates; green: largest reaction rates; values indicated in black are set equal to 0.

1st reaction partner	*Propagation*				*Termination*		
	$RO_2^\bullet + P$	$RO^\bullet + P$	$R^\bullet + P$	$RO_2^\bullet + RO_2^\bullet$	$RO_2^\bullet + RO_2^\bullet$	$RO_2^\bullet + R^\bullet$	$R^\bullet + RO_2^\bullet$
$R_{allyl,end}$	$2.0\ 10^{-9}$	0.0	$1.0\ 10^{-17}$		$1.5\ 10^{-10}$	$1.0\ 10^{-19}$	$1.0\ 10^{-19}$
$R_{allyl,mid}$	$1.5\ 10^{-8}$	0.0	$1.0\ 10^{-16}$		$7.0\ 10^{-9}$	$1.0\ 10^{-18}$	$1.0\ 10^{-18}$

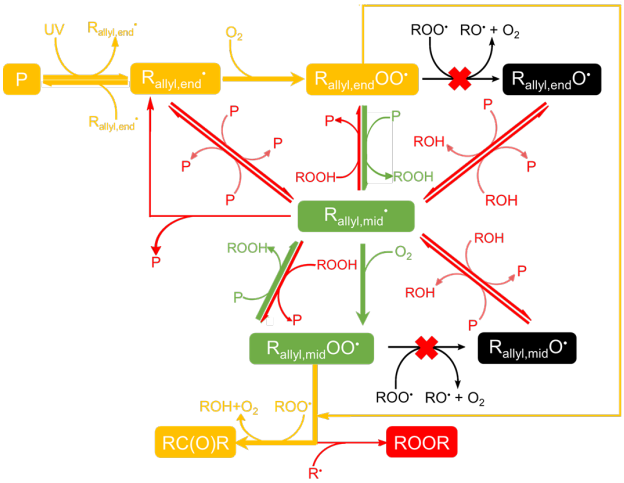

Figure 2. Reaction path analysis for autoxidation of poly(butadiene): reaction scheme shown for one polymer chain; colours according to reaction rates (red: lowest reaction rates; green: largest reaction rates; values indicated in black are set equal to 0) and thicker arrows indicate the dominant pathway

Simulations were repeated for a higher oxygen concentration ($100[O_2]_0$) and are summarised in the Supporting Information (see Figure S10 - S11 and Table S7). Surprisingly, Figure 3 shows that the decrease in number average chain length x_n as a function of time for $[O_2]_0$ and $100[O_2]_0$ coincide. The decrease in x_n as a function of time is used in this work as a measure for the autoxidation rate. Figure 2 shows a relatively high (green colour) rate for hydrogen abstraction of ROO, which does not benefit from a higher O_2 concentration. Hence, for PBD, the (slowest) initiation reaction is the rate determining step and the rates of the following reactions in the dominant reaction pathway stay the same, and the overall autoxidation rate is thus not influenced by a higher $[O_2]$. In the presence of increased oxygen, the reaction rates of the reactions involving alkyl radicals, which are very low in any case, do decrease due to the lower alkyl concentration. But otherwise the kinetic behaviour remains the same. Later on, it will be shown that this is not the same for PE and PIB.

Simulations were also performed for a higher initiation rate coefficient ($k_{ini} = 100k_{ini,0}$) to investigate if accelerated ageing conditions, characterized by a high UV intensity, have an influence on the dominant reaction pathway in the autoxidation mechanism (see Table S8, Figure S12-S13 Supporting Information). While each of the individual reaction rates, and the overall autoxidation rate, is higher, the dominant pathway does not change.

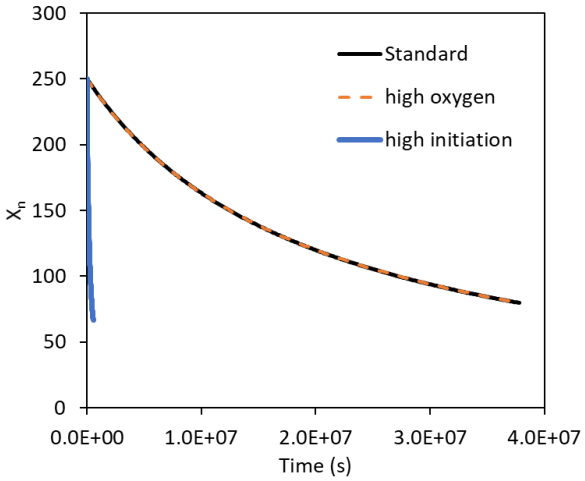

Figure 3. Decrease in number average chain length x_n as a function of time for poly(butadiene), representative for the autoxidation rate; as well as decrease in x_n in case of a higher oxygen concentration ($[O_2] = 100\ [O_2]_0$) and a higher initiation rate coefficient ($k_{ini} = 100\ k_{ini,0}$).

Poly(ethylene) (PE). For poly(ethylene), the reaction scheme and rate coefficients, as summarized in Table S5 in Supporting Information, are implemented in the *k*MC model. The reaction rates of the competitive reactions are summarized in Table 3 (see Figure S14 -S15 for more detail). Two radical types exist in the poly(ethylene) autoxidation mechanism, *viz* primary endchain and secondary midchain radicals. If we focus on their peroxyl radicals (after reaction with O_2), it can be seen in Table 3 that peroxyl termination is at least 2 orders of magnitude faster than its hydrogen abstraction. The autoxidation radicals are thus in PSS (pseudo steady-state; initiation rate = termination rate), but the BAS propagation reaction is slow. The autoxidation mechanism for PE is thus an "inefficient" chain reaction mechanism: chain length reduction mainly happens via the initiation reaction as only 1 out of 100 reaction steps for the peroxyl radicals is a hydrogen abstraction reaction, the rest are terminations. A slower autoxidation rate compared to poly(butadiene) is thus expected (see further). Midchain radicals, which are formed via hydrogen abstraction reactions, are thus not much formed explaining their low reaction rates in Table 3.

Table 3. Summary of *k*MC model output related to reaction rates (mol L^{-1} s^{-1}) of competitive reactions for poly(ethylene); reaction rate profiles as a function of time are given in Figure S14 and S15 in Supporting Information; red: lowest reaction rates; green: largest reaction rates; values indicated in black are set equal to 0.

1st reaction partner	*Propagation*				*Termination*		
	$RO_2^\bullet + P$	$RO^\bullet + P$	$R^\bullet + P$	$RO_2^\bullet + RO_2^\bullet$	$RO_2^\bullet + RO_2^\bullet$	$RO_2^\bullet + R^\bullet$	$R^\bullet + RO_2^\bullet$
$R_{prim,end}$	$8.0\ 10^{-12}$	0.0	$5.0\ 10^{-18}$		$7.5\ 10^{-10}$	$1.0\ 10^{-14}$	$5.0\ 10^{-14}$
$R_{sec,mid}$	$1.0\ 10^{-21}$	0.0	$5.0\ 10^{-17}$		$3.0\ 10^{-11}$	$1.0\ 10^{-26}$	$2.0\ 10^{-15}$

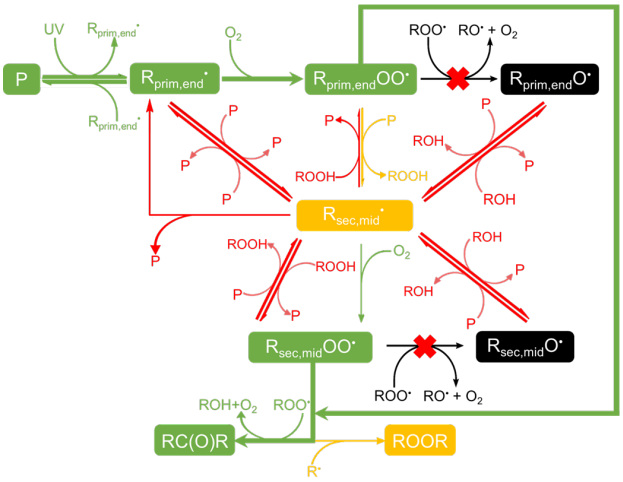

Figure 4. Reaction path analysis for autoxidation of poly(ethylene): reaction scheme shown for one polymer chain; colours according to reaction rates (red: lowest reaction rates; green: largest reaction rates; values indicated in black are set equal to 0) and thicker arrows indicate the dominant pathway.

The termination of primary and secondary peroxyl radicals leads to the formation of alcohols and aldehydes/ketones (see Scheme 3), and their dominant presence compared to ROOH (as a result of H abstraction of peroxyl radicals; main autoxidation product for PBD) in PE has been confirmed by IR,[43] by ^{17}O NMR,[44] and by ^{13}C NMR studies.[45, 46] It can be seen that also the termination rates of peroxyl radicals with alkyl radicals are higher compared to the poly(butadiene) case. In Figure 4, the reaction scheme (for one polymer chain) is summarized, where the dominant reaction pathway (composed of initiation/propagation/termination) is indicated by the thicker arrows. Primary radicals are formed via homolysis and react with oxygen (first two green thick arrows at the top). The resulting peroxyl radicals mostly terminate with each other (long thick green arrow at the right), prohibiting the transfer of the reactive centre to another polymer chain, forming a polymer alcohol and a polymer aldehyde (green box at the bottom left).

Unlike PBD, a higher oxygen concentration has an influence on the autoxidation rate, as can be seen in Figure 5, which shows the decrease in x_n as a function of time as a measure for the autoxidation rate. Instead of one dominant pathway as was the case for the lower oxygen concentration, now the dominant pathway changes as a function of time, as can be deduced from the changing slope of the x_n profile as a function of time. For the lower timescales, it can be seen that a higher oxygen concentration increases the autoxidation rate (faster decrease of x_n) due to a faster propagation of the primary endchain alkyl radicals with O_2. However, at larger timescales, it can be seen that autoxidation is slower in case of a higher oxygen concentration, hence oxygen serves as an inhibitor. This is because the competition for the primary endchain peroxyl radicals changes in favour of the hydrogen abstraction reaction (the difference between peroxyl termination and peroxyl H abstraction reaction rate in Table S9 in Supporting Information is only one order of magnitude, while in Table 3 the difference is two orders of magnitude). More secondary midchain radicals are thus formed, which mostly terminate. This last reaction pathway is slower compared to the original one, explaining the decrease in autoxidation rate.

The reaction rates of the individual reactions for a higher initiation rate coefficient (k_{ini} = 100$k_{ini,0}$) are given in Supporting Information (Figure S18 and S19 and summary in Table S10). It can be seen that again each of the individual reaction rates and the overall autoxidation rate is higher, but the dominant pathway does not change, as was also the case for PBD.

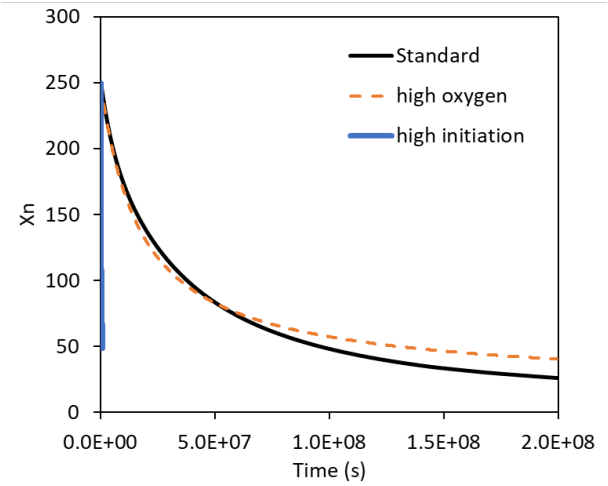

Figure 5. Decrease in number average chain length x_n as a function of time for poly(ethylene), representative for the autoxidation rate; as well as decrease in x_n in case of a higher oxygen concentration ($[O_2]$ = 100 $[O_2]_0$) and a higher initiation rate coefficient (k_{ini} = 100 $k_{ini,0}$).

Table 4. Summary of *k*MC model output related to reaction rates (mol L^{-1} s^{-1}) of competitive reactions for poly(isobutylene); reaction rate profiles as a function of time are given in Figure S20 to S22 in Supporting Information; red: lowest reaction rates; green: largest reaction rates; values indicated in black are set equal to 0.

1st reaction partner	*Propagation*				*Termination*		
	$RO_2^\bullet$ + P	$RO^\bullet$ + P	$R^\bullet$ + P	$RO_2^\bullet$ + $RO_2^\bullet$	$RO_2^\bullet$ + $RO_2^\bullet$	$RO_2^\bullet$ + $R^\bullet$	$R^\bullet$ + $RO_2^\bullet$
$R_{prim,end}$	6.0 10^{-15}	0.0	1.0 10^{-20}		8.0 10^{-10}	1.0 10^{-17}	6.0 10^{-18}
$R_{tert,end}$	7.0 10^{-13}	8.0 10^{-10}	5.0 10^{-15}	4.0 10^{-10}		3.0 10^{-18}	6.0 10^{-18}
$R_{sec,mid}$	5.0 10^{-17}	0.0	3.0 10^{-17}		8.0 10^{-10}	3.0 10^{-21}	6.0 10^{-18}

Poly(isobutylene) (PIB). For poly(isobutylene), the reaction scheme and rate coefficients, as summarized in Table S6 in Supporting Information are implemented in the *k*MC model. The reaction rates of the competitive reactions are summarized in Table 4 (see Figure S20 - S22 in the Supporting Information for more detail). For PIB, three radical types are formed during autoxidation: primary end-, secondary mid- and tertiary endchain radicals. Two of these types, primary and tertiary radicals, are produced in the initiation reaction for PIB. As two different radical types are formed upon initiation, a more complex autoxidation behaviour than for PBD and PE results. There are now two dominant pathways, one for each initiating radical type. Table 4 shows that the fastest reaction is different for both initiating radical types: after their peroxyl radicals are formed by the reaction with oxygen, primary peroxyl radicals mainly terminate (green cell in first row in Table 4). Contrary, tertiary peroxyl radicals mainly propagate via the formation of alkoxyl radicals ($RO^\bullet$) (second green cell in second row in Table 4), which are very reactive towards hydrogen abstraction (first green cell in second row in Table 4). The third radical type, being secondary midchain radicals, are formed via hydrogen abstraction reactions and, after reacting with oxygen, will mostly terminate (green cell in third row in Table 4).

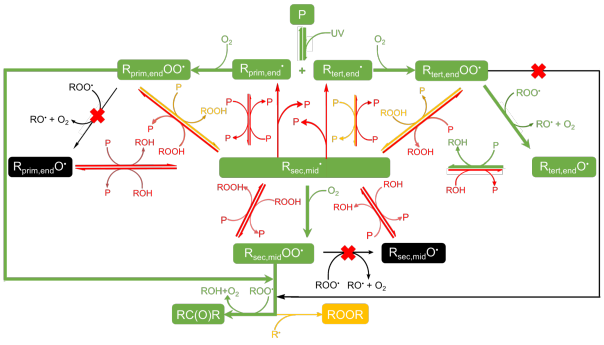

Figure 6. Reaction path analysis for autoxidation of poly(isobutylene): reaction scheme shown for one polymer chain; two types of radicals are formed during initiation, leading to two different dominant pathways; colours according to reaction rates (red: lowest reaction rates; green: largest reaction rates; values indicated in black are set equal to 0) and thicker arrows indicate the dominant pathway.

In Figure 6, the reaction scheme (for one polymer chain) is summarized where the dominant reaction pathway for each of the two radical types formed upon initiation (composed of initiation/propagation/termination) is indicated by the thicker arrows. Both the primary and tertiary radical formed upon initiation first react with oxygen (green thick arrows at the top facing left and right respectively). Primary peroxyl radicals then immediately terminate (long green arrow at the left), while tertiary peroxyl radicals propagate to tertiary alkoxyl radicals that undergo hydrogen abstraction with the formation of secondary midchain radicals (oblique thick green arrow and horizontal thick green arrow on the right). Secondary midchain radicals (green box in centre) react with oxygen, forming peroxyl midchain radicals, which mainly terminate (thick green arrow in bottom centre part), as confirmed from Table 4.

A higher oxygen concentration does not significantly change the autoxidation rate for PIB, as shown in Figure 7. The rates of the individual reactions for $[O_2] = 100[O_2]_0$ are shown in Figure S23 to S25 and summarized in Table S11 in Supporting Information. Only a small acceleration in the reduction of x_n as a function of time (full line *vs.* dashed line in Figure 7a) and hence a small increase in the autoxidation rate, is observed. For the pathway of the primary end radicals formed upon initiation, we see the same change in behaviour in case of a higher oxygen concentration as for PE. The competition between termination and hydrogen abstraction for the primary peroxyl radicals changes in favour of the hydrogen abstraction reaction, decreasing the autoxidation rate (see further). For the tertiary radicals formed upon initiation, an increase in the reaction rate of alkoxyl tertiary radical formation is observed in Table S11 compared to Table 4 and the same for the reaction rate of hydrogen abstraction by the alkoxyl radical. An increase in oxygen concentration for the tertiary radical thus leads to an increase in autoxidation rate. Overall, the increase in autoxidation rate is a bit stronger than the decrease, so that a small increase in the autoxidation rate results in Figure 7.

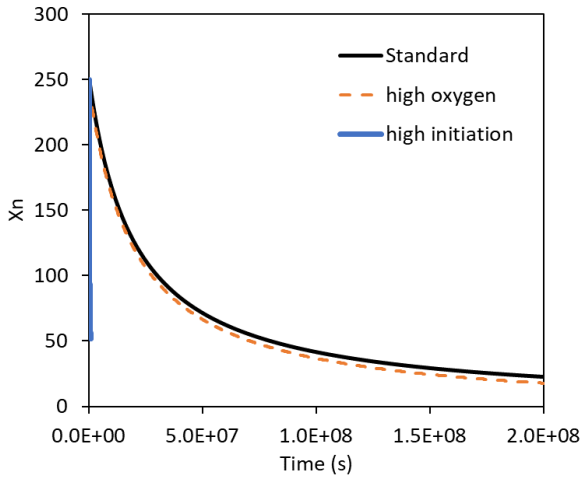

Figure 7. Decrease in number average chain length x_n as a function of time for poly(isobutylene), representative for the autoxidation rate; as well as decrease in x_n in case of a higher oxygen concentration ($[O_2] = 100\ [O_2]_0$) and a higher initiation rate coefficient ($k_{ini} = 100\ k_{ini,0}$).

The reaction rates of the individual reactions for a higher initiation rate coefficient (k_{ini} = 100$k_{ini,0}$) are given in Supporting Information (Figure S26 to S28 and summary in Table S12). Similar to PBD and PE, it can be seen that each of the individual reaction rates is higher, as is the overall autoxidation rate (see Figure 7 bottom), but the dominant pathway does not change.

Comparison. In Figure 8, the decrease in average chain length x_n as a function of time is compared for the three model polymers considered in this work as a measure for their respective autoxidation rate. It can be seen that the slowest autoxidation rate is observed for poly(ethylene) (slowest decrease in x_n as a function of time), poly(isobutylene) degrades at an intermediate rate and poly(butadiene) degrades the fastest (fastest decrease in x_n as a function of time). This is in agreement with low-temperature studies of the thermooxidation of PIB[47, 48], which suggested that oxidation of PIB is faster compared to similar studies of PE.[49, 50] Overall, quaternary (random) defects in polymer chains are expected to accelerate the autoxidation mechanism more than unsaturated defects. This is logical because in PIB (containing a quaternary defect per repeating unit) each homolysis event leads to a primary and a tertiary radical following a different dominant pathway, while for PBD (containing an unsaturated defect per repeating unit), homolysis leads to two allylic radicals. Structural defects in polymer chains have thus a magnifying effect on polymer degradation *via* autoxidation because the dominant radicals, *i.e.* peroxyl radicals for PBD and alkoxyl radicals for PIB, have a high reactivity towards propagation, *i.e.* hydrogen transfer, reactions.

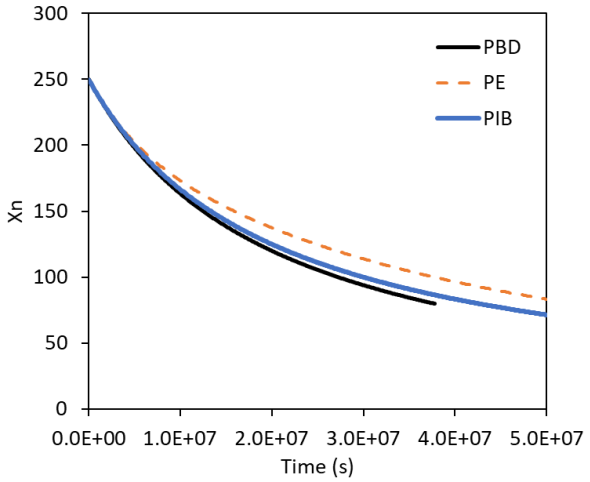

Figure 8. Decrease in number average chain length x_n as a function of time for poly(ethylene) (blue), poly(butadiene) (orange) and poly(isobutylene) (grey) for $[O_2]_0$ and $k_{ini,0}$.

CONCLUSIONS

Understanding the mechanisms involved in the degradation of polymers is crucial in improving their resistance to environmental aging and in understanding how to design accelerated aging studies that are reflective of chemical conditions found in the environments in which the polymers are to be used. In this work, a kinetic Monte Carlo (*k*MC) model is developed to predict the dominant reaction pathway of polymers in the presence of oxygen and to study the effect of structural motifs (unsaturations and quaternary carbon atoms) in the polymer structure. This is done for three model polymers, namely poly(butadiene), poly(ethylene) and poly(isobutylene). Kinetic studies are indispensable to assess the relative contribution of the different reaction pathways under given conditions.

Based on the kinetic study performed in this work, it is confirmed that the autoxidation mechanisms of poly(butadiene) agree with the mechanism as described by the basic autoxidation scheme (BAS). For poly(ethylene), the autoxidation mechanism is an inefficient chain reaction mechanism due to the low hydrogen abstraction rates of the peroxyl radicals and, hence, reduction in the average chain length, x_n, mainly occurs via the initiation reaction. The autoxidation is thus slower compared to poly(butadiene) due to the dominant role of peroxyl radical termination, which is absent in poly(butadiene). Contrary, autoxidation of poly(isobutylene) occurs via formation of reactive alkoxyl radials that result from peroxyl termination, and the alkoxyl radicals then propagate damage via subsequent hydrogen abstraction reaction. The presence of quaternary carbons leads to an increase in autoxidation rate compared to poly(ethylene).

The role of oxygen in autoxidation is more complex than it first appears. For unsaturated polymers, the *k*MC model is unaffected by the oxygen concentration within the range studied. For saturated polymers without quaternary defects, autoxidation is inhibited to some extent by oxygen due to the formation of unreactive peroxyl radicals. For saturated polymers with quaternary defects, an increase in oxygen concentration leads to the faster formation of reactive alkoxyl radicals and thus increases the autoxidation rate.

Increasing the initiation rate coefficient in the *k*MC model, in order to simulate accelerated ageing conditions (*e.g.* due to a stronger UV irradiation), has no influence on the relative contribution of the competitive reaction pathways. An increase of the autoxidation rate proportional to the increase of the initiation rate coefficient is predicted.

The work demonstrates that unsaturated groups and quaternary units compromise the stability of polymers. Hence, the current work provides the first kinetic framework to assess the lasting impact, in terms of duration, of solid plastic (waste) in atmospheric conditions on the environment, for a variety of polymers and often-encountered defects such as unsaturations and branches in common polymer materials. These defects should thus be minimized to counteract aging under UV-exposure, or conversely, they should be incorporated when accelerated autoxidation is desirable.

ASSOCIATED CONTENT

Supporting Information

Complete computational and kinetic modeling details. The Supporting Information is available free of charge on the ACS Publications website.

Corresponding Author

*Email: paul.vanSteenberge@ugent.be; michelle.coote@anu.edu.au

ACKNOWLEDGMENT

The authors acknowledge financial support from the Australian Research Council (ARC) Centre of Excellence for Electromaterials Science, an ARC Laureate Fellowship (to M.L.C.), and generous supercomputing time from the National Computational Infrastructure. GG gratefully

acknowledges Ms. Anna Piras and the state of Baden-Württemberg through bwHPC (JUSTUS 2) for computational resources and assistance. P.H.M.V.S acknowledges FWO through a postdoctoral fellowship.

Funding Sources

Australian Research Council (FL170100041, CE140100012)

REFERENCES

(1) Laycock, B.; Nikolic, M.; Colwell, J. M.; Gauthier, E.; Halley, P.; Bottle, S.; George, G. Lifetime prediction of biodegradable polymers. Prog. Polym. Sci. 2017, 71, 144-189.

(2) Bolland, J. L. Kinetic studies in the chemistry of rubber and related materials. I. The thermal oxidation of ethyl linoleate. Proc R Soc Lon Ser. A 1946, 186, 218-236.

(3) Bolland, J. L. Kinetic studies in the chemistry of rubber and related materials. VI. The benzoyl peroxide-catalysed oxidation of ethyl linoleate. Trans. Faraday Soc. 1948, 44, 669-677.

(4) Bolland, J. L.; Gee, G. Kinetic studies in the chemistry of rubber and related materials. II. The kinetics of oxidation of unconjugated olefins. Trans. Faraday Soc. 1946, 42, 236-243.

(5) Bolland, J. L.; Gee, G. Kinetic studies in the chemistry of rubber and related materials. III. Thermochemistry and mechanisms of olefin oxidation. Trans. Faraday Soc. 1946, 42, 244-252.

(6) Bolland, J. L.; Tenhave, P. Kinetic studies in the chemistry of rubber and related materials. IV. The inhibitory effect of hydroquinone on the thermal oxidation of ethyl linoleate. Trans. Faraday Soc. 1947, 43, 201-210.

(7) Yin, H.; Xu, L.; Porter, N. A. Free Radical Lipid Peroxidation: Mechanisms and Analysis. Chemical Reviews 2011, 111 (10), 5944-5972. DOI: 10.1021/cr200084z.

(8) Audouin, L.; Achimsky, L.; Verdu, J. Kinetic modelling of low temperature oxidation of hydrocarbon polymers. Handbook of Polymer Degradation 2000, 727-763.

(9) Zweifel, H.; Maier, R. D.; Schiller, M. Plastics Additives Handbook; Hanser Publications, 2009.

(10) Gryn'ova, G.; Hodgson, J. L.; Coote, M. L. Revising the mechanism of polymer autooxidation. Org. Biomol. Chem. 2011, 9 (2), 480-490, Article. DOI: 10.1039/c0ob00596g.

(11) Lee, R.; Coote, M. L. New insights into 1,2,4-trioxolane stability and the crucial role of ozone in promoting polymer degradation. Phys. Chem. Chem. Phys. 2013, 15 (39), 16428-16431, Article. DOI: 10.1039/c3cp52863d.

(12) Lee, R.; Coote, M. L. Mechanistic insights into ozone-initiated oxidative degradation of saturated hydrocarbons and polymers. Phys. Chem. Chem. Phys. 2016, 18 (35), 24663-24671, Article. DOI: 10.1039/c6cp05064f.

(13) Lee, R.; Gryn'ova, G.; Ingold, K. U.; Coote, M. L. Why are sec-alkylperoxyl bimolecular self-reactions orders of magnitude faster than the analogous reactions of tert-alkylperoxyls? The unanticipated role of CH hydrogen bond donation. Phys. Chem. Chem. Phys. 2016, 18 (34), 23673-23679, Article. DOI: 10.1039/c6cp04670c.

(14) Smith, L. M.; Aitken, H. M.; Coote, M. L. The Fate of the Peroxyl Radical in Autoxidation: How Does Polymer Degradation Really Occur? Accounts of Chemical Research 2018, 51 (9), 2006-2013, Review. DOI: 10.1021/acs.accounts.8b00250.

(15) Starnes Jr., W. H. Structural defects in poly(vinyl chloride). Journal of Polymer Science Part A: Polymer Chemistry 2005, 43 (12), 2451-2467. DOI: 10.1002/pola.20811.

(16) Kelsey, D. R.; Kiibler, K. S.; Tutunjian, P. N. Thermal stability of poly(trimethylene terephthalate). Polymer 2005, 46 (21), 8937-8946. DOI: https://doi.org/10.1016/j.polymer.2005.07.015.

(17) Hirata, T.; Kashiwagi, T.; Brown, J. E. Thermal and oxidative degradation of poly(methyl methacrylate): weight loss. Macromolecules 1985, 18 (7), 1410-1418. DOI: 10.1021/ma00149a010.

(18) Kashiwagi, T.; Inaba, A.; Brown, J. E.; Hatada, K.; Kitayama, T.; Masuda, E. Effects of weak linkages on the thermal and oxidative degradation of poly(methyl methacrylates). Macromolecules 1986, 19 (8), 2160-2168. DOI: 10.1021/ma00162a010.

(19) Peterson, J. D.; Vyazovkin, S.; Wight, C. A. Kinetic Study of Stabilizing Effect of Oxygen on Thermal Degradation of Poly(methyl methacrylate). The Journal of Physical Chemistry B 1999, 103 (38), 8087-8092. DOI: 10.1021/jp991582d.

(20) Bennet, F.; Lovestead, T. M.; Barker, P. J.; Davis, T. P.; Stenzel, M. H.; Barner-Kowollik, C. Degradation of Poly(methyl methacrylate) Model Compounds at Constant Elevated Temperature Studied via High Resolution Electrospray Ionization Mass Spectrometry (ESI-MS). Macromolecular Rapid Communications 2007, 28 (16), 1593-1600. DOI: 10.1002/marc.200700330.

(21) Soeriyadi, A. H.; Trouillet, V.; Bennet, F.; Bruns, M.; Whittaker, M. R.; Boyer, C.; Barker, P. J.; Davis, T. P.; Barner-Kowollik, C. A detailed surface analytical study of degradation processes in (meth)acrylic polymers. Journal of Polymer Science Part A: Polymer Chemistry 2012, 50 (9), 1801-1811. DOI: 10.1002/pola.25947.

(22) Gardette, J.-L.; Lemaire, J. Photothermal and thermal oxidations of rigid, plasticized and pigmented poly(vinyl chloride). Polymer Degradation and Stability 1991, 34 (1), 135-167. DOI: https://doi.org/10.1016/0141-3910(91)90117-A.

(23) Gardette, M.; Perthue, A.; Gardette, J.-L.; Janecska, T.; Földes, E.; Pukánszky, B.; Therias, S. Photo- and thermal-oxidation of polyethylene: Comparison of mechanisms and influence of unsaturation content. Polymer Degradation and Stability 2013, 98 (11), 2383-2390. DOI: https://doi.org/10.1016/j.polymdegradstab.2013.07.017.

(24) Tracy, J.; D'hooge, D. R.; Bosco, N.; Delgado, C.; Dauskardt, R. Evaluating and predicting molecular mechanisms of adhesive degradation during field and accelerated aging of photovoltaic modules. Progress in Photovoltaics: Research and Applications 2018, 26 (12), 981-993. DOI: 10.1002/pip.3045.

(25) Gillespie, D. T. A general method for numerically simulating the stochastic time evolution of coupled chemical reactions. Journal of computational physics 1976, 22 (4), 403-434.

(26) Gillespie, D. T. Exact stochastic simulation of coupled chemical reactions. The Journal of Physical Chemistry 1977, 81 (25), 2340-2361. DOI: 10.1021/j100540a008.

(27) Van Steenberge, P. H. M.; D'hooge, D. R.; Wang, Y.; Zhong, M.; Reyniers, M.-F.; Konkolewicz, D.; Matyjaszewski, K.; Marin, G. B. Linear Gradient Quality of ATRP Copolymers. Macromolecules 2012, 45 (21), 8519-8531. DOI: 10.1021/ma3017597.

(28) Van Steenberge, P. H. M.; D'hooge, D. R.; Reyniers, M. F.; Marin, G. B. Improved kinetic Monte Carlo simulation of chemical composition-chain length distributions in polymerization processes. Chemical Engineering Science 2014, 110, 185-199. DOI: https://doi.org/10.1016/j.ces.2014.01.019.

(29) Izgorodina, E. I.; Lin, C. Y.; Coote, M. L. Energy-directed tree search: an efficient systematic algorithm for finding the lowest energy conformation of molecules. Phys. Chem. Chem. Phys. 2007, 9, 2507-2516.

(30) Curtiss, L. A.; Raghavachari, K.; Redfern, P. C.; Baboul, A. G.; Pople, J. A. Gaussian-3 theory using coupled cluster energies. Chemical Physics Letters 1999, 314 (1), 101-107. DOI: https://doi.org/10.1016/S0009-2614(99)01126-4.

(31) Merrick, J. P.; Moran, D.; Radom, L. An Evaluation of Harmonic Vibrational Frequency Scale Factors. The Journal of Physical Chemistry A 2007, 111 (45), 11683-11700. DOI: 10.1021/jp073974n.

(32) Levchik, S. V.; Weil, E. D. A review on thermal decomposition and combustion of thermoplastic polyesters. Polymers for Advanced Technologies 2004, 15 (12), 691-700.

(33) Scott, G. Initiation processes in polymer degradation. Polymer degradation and stability 1995, 48 (3), 315-324.

(34) Roberfroid, M. B. Free radicals and oxidation phenomena in biological systems; M. Dekker, 1995.

(35) François-Heude, A.; Richaud, E.; Desnoux, E.; Colin, X. A general kinetic model for the photothermal oxidation of polypropylene. Journal of Photochemistry and Photobiology A: Chemistry 2015, 296, 48-65. DOI: https://doi.org/10.1016/j.jphotochem.2014.08.015.

(36) Maillard, B.; Ingold, K. U.; Scaiano, J. C. Rate constants for the reactions of free radicals with oxygen in solution. Journal of the American Chemical Society 1983, 105 (15), 5095-5099. DOI: 10.1021/ja00353a039.

(37) Wagner, A. F.; Slagle, I. R.; Sarzynski, D.; Gutman, D. Experimental and theoretical studies of the ethyl+ oxygen reaction kinetics. Journal of Physical Chemistry 1990, 94 (5), 1853-1868.

(38) Gryn'ova, G.; Hodgson, J. L.; Coote, M. L. Revising the mechanism of polymer autooxidation. Organic & Biomolecular Chemistry 2011, 9 (2), 480-490, 10.1039/C0OB00596G. DOI: 10.1039/C0OB00596G.

(39) Hernández-Ortiz, J. C.; Van Steenberge, P. H. M.; Reyniers, M.-F.; Marin, G. B.; D'hooge, D. R.; Duchateau, J. N. E.; Remerie, K.; Toloza, C.; Vaz, A. L.; Schreurs, F. Modeling the reaction event history and microstructure of individual macrospecies in postpolymerization

modification. AIChE Journal 2017, 63 (11), 4944-4961. DOI: 10.1002/aic.15842.
(40) Epacher, E.; Tolvéth, J.; Kröhnke, C.; Pukánszky, B. Processing stability of high density polyethylene: effect of adsorbed and dissolved oxygen. Polymer 2000, 41 (23), 8401-8408. DOI: https://doi.org/10.1016/S0032-3861(00)00191-9.
(41) François-Heude, A.; Richaud, E.; Guinault, A.; Desnoux, E.; Colin, X. Impact of Oxygen Transport Properties on Polypropylene Thermal Oxidation, Part 1: Effect of Oxygen Solubility. *J. Appl. Polym. Sci.* **2014**, *132*, 1-16.
(42) Li, H.; Tung, K. K.; Paul, D. R.; Freeman, B. D.; Stewart, M. E.; Jenkins, J. C. Characterization of Oxygen Scavenging Films Based on 1,4-Polybutadiene. *Ind. Eng. Chem. Res.* **2012**, *51* (21), 7138-7145. DOI: 10.1021/ie201905j.
(43) Lacoste, J.; Carlsson, D. J. Gamma-, photo-, and thermally-initiated oxidation of linear low density polyethylene: A quantitative comparison of oxidation products. *Journal of Polymer Science Part A: Polymer Chemistry* **1992**, *30* (3), 493-500. DOI: 10.1002/pola.1992.080300316.
(44) Alam, T. M.; Celina, M.; Assink, R. A.; Clough, R. L.; Gillen, K. T.; Wheeler, D. R. Investigation of Oxidative Degradation in Polymers Using 17O NMR Spectroscopy. *Macromolecules* **2000**, *33* (4), 1181-1190. DOI: 10.1021/ma991061o.
(45) Assink, R. A.; Celina, M.; Dunbar, T. D.; Alam, T. M.; Clough, R. L.; Gillen, K. T. Analysis of hydroperoxides in solid polyethylene by MAS 13C NMR and EPR. *Macromolecules* **2000**, *33* (11), 4023-4029.
(46) Jelinski, L. W.; Dumais, J. J.; Luongo, J. P.; Cholli, A. L. Thermal oxidation and its analysis at low levels in polyethylene. *Macromolecules* **1984**, *17* (9), 1650-1655. DOI: 10.1021/ma00139a002.
(47) Pazur, R. J. Activation energy of poly(isobutylene) under thermo-oxidative conditions from 40 to 100 °C. *Polymer Degradation and Stability* **2014**, *104*, 57-61. DOI: https://doi.org/10.1016/j.polymdegradstab.2014.03.028.
(48) Gonon, L.; Troquet, M.; Fanton, E.; Gardette, J.-L. Thermo and photo-oxidation of polyisobutylene—II. Influence of the temperature. *Polymer Degradation and Stability* **1998**, *62* (3), 541-549. DOI: https://doi.org/10.1016/S0141-3910(98)00040-8.
(49) Chirinos-Padrón, A. J.; Hernández, P. H.; Chávez, E.; Allen, N. S.; Vasiliou, C.; DePoortere, M. Influences of unsaturation and metal impurities on the oxidative degradation of high density polyethylene. *European Polymer Journal* **1987**, *23* (12), 935-940. DOI: https://doi.org/10.1016/0014-3057(87)90036-X.
(50) Allen, N. S.; Edge, M.; Holdsworth, D.; Rahman, A.; Catalina, F.; Fontan, E.; Escalona, A. M.; Sibon, F. F. Ageing and spectroscopic properties of polyethylenes: comparison with metallocene polymer. *Polymer Degradation and Stability* **2000**, *67* (1), 57-67. DOI: https://doi.org/10.1016/S0141-3910(99)00121-4.